Wave-packet analysis of laser-induced half-collision processes

F. H. Mies
National Institute of Standards and Technology, Gaithersburg, Maryland 20899

A. Giusti-Suzor
Laboratoire de Chimie-Physique, 11 rue Pierre et Marie Curie, 75231 Paris, France

(Received 8 July 1991)

The usual approach to calculating multiphoton collision and half-collision processes uses the interaction picture and introduces a classical time-dependent field into the Hamiltonian for the scattered particles, which is further simplified using the Floquet ansatz. In particular, the laser-induced decay of an initial bound state is derived from a *half-collision* Floquet ansatz that utilizes a *complex* quasienergy, whose imaginary part is identified with the laser-induced decay constant of the bound state. This interpretation presupposes a pure exponential decay of the initial-state population and yields a Lorentzian distribution of product-state energies in the infinite-depletion limit. Here we demonstrate how a *full-collision* Floquet ansatz can be derived from a fully quantal wave packet constructed to represent scattering in the presence of a coherent state of the laser field. The wave packet utilizes the set of the time-independent close-coupled wave functions for scattering in the field generated by quantized radiation number states. The resultant Floquet scattering states are energy normalized and stationary, and the quasienergy is real. We show how to use these states to construct a coherent-state wave packet that describes the decay of an arbitrarily prepared bound state, and yields a *half-collision* Floquet ansatz without any commitment to a complex quasienergy. The product energy and quantum-state distribution in the infinite-depletion limit are obtained without approximation to exponential decay. Further we show how the Fourier transform of the infinite-depletion line shape gives the temporal behavior of the initial bound-state population, often with distinctly nonexponential behavior. Such results are demonstrated for the above-threshold ionization of H, and the above-threshold dissociation of H_2^+. In the following paper [R. W. Heather and F. H. Mies, Phys. Rev. **44**, XXXX (1991)], excellent agreement is found between the present fully quantal wave-packet approach, utilizing the time-independent scattering wave functions, and the comparable solutions to the time-dependent Schrödinger equation for a corresponding classical time-dependent laser field.

PACS number(s): 32.80.Wr

I. INTRODUCTION

Nonperturbative treatments of multiphoton ionization (MPI) of atoms [1–5], e.g.,

$$\mathrm{H}+n\hbar\omega\rightarrow\mathrm{H}^{+}+e \tag{1}$$

and multiphoton dissociation (MPD) of diatoms [6–9], e.g.,

$$\mathrm{H}_2^{+}+n\hbar\omega\rightarrow\mathrm{H}^{+}+\mathrm{H} \tag{2}$$

generally proceed from a classical description of an intense single-mode laser defined by the time-dependent vector potential

$$\overline{\mathbf{A}}(\mathbf{x},t)=\frac{c}{\omega}\overline{\mathbf{E}}\cos(\omega t-\mathbf{k}_{\omega}\cdot\mathbf{x}+\phi)\ . \tag{3}$$

Heather and Metiu [8] and Bardsley, Szöke, and Comella [3] have solved the resultant time-dependent Schrödinger equation for MPD and MPI, respectively, using split-operator techniques. Such procedures are imperative for femtosecond pulsed lasers where the electric field amplitude $\overline{\mathbf{E}}(t)$ varies rapidly with time over the course of the scattering event.

Alternatively, if we can assume that the amplitude of the electric field $\overline{\mathbf{E}}\equiv(8\pi\hbar\omega\overline{N}/V)^{1/2}\hat{\mathbf{e}}$, or equivalently the effective number of photons $\overline{N}$ contained in the volume V, is constant in time [10], the periodic time dependence can be exploited in the following *half-collision* Floquet ansatz [11] to describe the decay of some initial bound state i which is subject to this classical field at $t=0$. This can be represented as follows:

$$\overline{\Psi}_i(\overline{E}_i,\mathbf{x},R;t)\approx\left[\sum_{n'=-\infty}^{+\infty}\overline{\Psi}_{n',i}(\mathbf{x},R)e^{-in'(\omega t+\phi)}\right]\times e^{-i\overline{E}_i t/\hbar} \tag{4}$$

where the quasienergy $\overline{E}_i=E_i^0+\overline{\Delta}_i-i\overline{\Gamma}_i$ is taken as complex [12]. The quantity $\overline{\Delta}_i$ is interpreted as the laser-induced shift relative to the unperturbed initial eigenvalue E_i^0, and $\Gamma_i/\hbar$ is interpreted as the laser-induced rate of decay of the initial state. Appropriate outgoing boundary conditions must be imposed on the functions $\overline{\Psi}_{n,i}$ as $R\rightarrow\infty$, where R is the magnitude of either the electron coordinate in Eq. (1) or the internuclear coordinate in Eq. (2), and $\mathbf{x}$ represents all the remaining degrees of freedom.

In order to avoid a commitment to a purely exponential decay implied by the complex quasienergy, we will show how to construct a proper decaying wave packet for initial bound state $\bar{\Psi}_i$ using a complete set of Floquet scattering states. The following *full-collision* Floquet ansatz [2,13] can be used to describe any type of scattering in the presence of a classical field,

$$\bar{\Psi}^{+}_{n\gamma}(E,\mathbf{x},R;t)=\left[\sum_{n'=-\infty}^{+\infty}\sum_{\gamma'}\psi_{\gamma'}(\mathbf{x})\bar{F}_{n'\gamma',n\gamma}(E,R)\times e^{-in'(\omega t+\phi)}\right]e^{-iEt/\hbar}. \quad (5)$$

The incoming state $\bar{\Psi}^{+}_{n\gamma}(E,\mathbf{x},R;t)$ is a particular time-dependent solution of the total Hamiltonian, expanded in a set of channel states [14] ψ_γ appropriate to processes (1) or (2). Typical incoming scattering boundary conditions are applied to the matrix of *time-independent* radial solution vectors $\bar{\mathbf{F}}(E,R)$ which are obtained numerically from close-coupled scattering codes. Since the bracketed portion of Eq. (5) is perfectly periodic in time, i.e., $\bar{\Psi}(E,t)\rightarrow\bar{\Psi}(E,t+2\pi m/\omega)$, the parameter E is referred to as a "quasienergy" and solutions can only be uniquely specified within multiples of the photon energy [11], i.e., $\bar{\Psi}(E,t)\rightarrow\bar{\Psi}(E+m\hbar\omega,t)$. However, the radial functions are chosen to be energy normalized, and the quasienergy E is *real*. The parameter n' is the Floquet index and indicates the number of photons absorbed ($n'-n>0$) or emitted ($n'-n<0$) relative to the *initial* scattering state incident in channel γ in a field with mean number $\bar{N}-n$.

We have two objectives in this paper. The first is to derive the full-collision Floquet ansatz (5) using a completely quantum approach for both the radiation field and the scattering. The second is to use the same approach to construct the half-collision Floquet ansatz (4) corresponding to the photodissociation or photoionization of some prescribed initial bound state which is abruptly subjected to the time-dependent field (3) at $t=0$. Using the full-collision solutions to construct a proper decaying wave packet we avoid any commitment to the complex quasienergy approximation. We will use the specific MPD and MPI processes in (1) and (2) to demonstrate that the half-collision Floquet ansatz is not restricted to isolated, exponentially decaying states.

The analysis we employ is outlined schematically in Table I. Everything is accomplished using the complete set of *either* incoming (+) or outgoing (−) close-coupled field-dressed scattering states $\Omega^{\pm}_{n\gamma}(E,N,t)$ as a basis. These describe a full-collision process occurring in a field represented by quantized number states $|N\rangle$. Since $|N\rangle$ is an exact energy eigenfunction, the total energy of the colliding system is conserved, and $\Omega^{\pm}_{n\gamma}$ can be constructed from *time-independent,* close-coupled scattering wave functions, with E real. As a corollary the complete set of outgoing scattering wave functions $\Omega^{-}_{n\gamma}$ can be used to construct a fully quantized wave packet $\Omega_i(N,t)$ for a *half-* collision process in quantized field.

Using arguments first presented by Shirley [15] in his original derivation of the Floquet theory for a two-level system, the classical expression (5) for a full-collision process can be derived using a quantal description of the

TABLE I. Schematic of theoretical analysis. (A) The time-independent close-coupled solutions for scattering of particles $A(\gamma)+B(\gamma)$ in an incident laser field represented by the number state $|N-n\rangle$, are used to construct the in (+) or out (−) quantal field plus full-collision wave packet $\Omega^{\pm}_{n\gamma}(E,N,t)$ in Sec. II. (B) A half-collision wave packet $\Omega_i(N,t)$ is constructed in Sec. III which represents decay of an initial bound state $AB(i)$ atom or molecule induced by the quantal radiation field $|N-n\rangle$. (C) A Poisson distribution of number state packets is used in Sec. IV to construct an incident coherent radiation state $|\bar{\alpha}\rangle$ and an expression for the full-collision Floquet state $\bar{\Psi}^{\pm}_{n\gamma}(E,t)$ is obtained. (D) Starting with either (B) or (C) a half-collision wave packet for decay of $AB(i)$ in a coherent radiation field is constructed and a half-collision Floquet state Ψ_i is defined at the conclusion of Sec. IV.

(A)

Quantal-field plus full-collision wave packet

$$A(\gamma)+B(\gamma)+(N-n)\hbar\omega\rightarrow A(\gamma')+B(\gamma')+(N-n')\hbar\omega$$
$$\Omega^{\pm}_{n\gamma}(E,N,t)$$

(B)

Quantal-field plus half-collision wave packet

$$AB(i)+N\hbar\omega\rightarrow A(\gamma)+B(\gamma)+(N-n)\hbar\omega$$
$$\Omega_i(N,t)=\sum_{n\gamma}\int dEC_{n\gamma\leftarrow i}(E,N)\Omega^{-}_{n\gamma}(E,N,t)$$

(C)

(Coherent state) × (full Floquet state)

$$A(\gamma)+B(\gamma)+|\bar{\alpha}\rangle\rightarrow A(\gamma')+B(\gamma')-(n'-n)\hbar\omega+|\bar{\alpha}\rangle$$
$$|\bar{\alpha}\rangle\bar{\Psi}^{\pm}_{n\gamma}=\sum_{N}\bar{c}(N)\Omega^{\pm}_{n\gamma}(E,N,t)$$

(D)

(Coherent state) × (half Floquet state)

$$AB(i)+|\bar{\alpha}\rangle\rightarrow A(\gamma)+B(\gamma)-n\hbar\omega+|\bar{\alpha}\rangle$$
$$|\bar{\alpha}\rangle\bar{\Psi}_i(t)=\sum_{N}\bar{c}(N)\sum_{n\gamma}\int dEC_{n\gamma\leftarrow i}(E,N)\Omega^{-}_{n\gamma}(E,N,t)$$
$$\approx|\bar{\alpha}\rangle\sum_{n\gamma}\int dEC_{n\gamma\leftarrow i}(E,\bar{N})\bar{\Psi}^{-}_{n\gamma}(E,t)$$

laser expanded in a complete set of photon number states $|N\rangle$. The exact close-coupled scattering wave functions $\Omega^{+}_{n\gamma}(N,E,t)$ are combined to form a wave packet incident in a pure *coherent* radiation state [15–17]

$$|\bar{\alpha}(t)\rangle = \sum_{N=0}^{\infty} e^{-|\bar{\alpha}|^2} \frac{(\bar{\alpha})^N}{\sqrt{N!}} e^{-iN\omega t}|N\rangle \tag{6}$$

which leads to the quantal representation of the classical field (3) if we choose $\bar{\alpha}=e^{-i\phi}\sqrt{\bar{N}}$, where $\bar{N}=|\bar{E}|^2V/(8\pi\hbar\omega)$ [12]. Assuming that $\bar{N}$ is sufficiently large, the resultant packet factors as $|\bar{\alpha}(t)\rangle\bar{\Psi}^{+}_{n\gamma}(E,t)$ and yields the expression (5). In this case E still remains real. Using these full-collision Floquet solutions we can also construct a half-collision wave packet subjected to the classical time-dependent field (3) at $t=0$. Again we obtain a factorization $|\bar{\alpha}(t)\rangle\bar{\Psi}_i(t)$ which defines the half-collision Floquet expression comparable to (4), but *without* any introduction of a complex quasienergy.

Aside from the pleasing feature of unifying the two approaches, the quantal derivation gives us a rigorous basis for extracting observable macroscopic properties from the Floquet ansatz, allows us to use the full apparatus of quantal scattering codes, and avoids the limitations imposed by the usual complex-quasienergy algorithms which assume all line-shape profiles are Lorentzian as prescribed by a pure exponential decay of the initial bound state. In particular we will show how the distribution of final channel states, in the limit of infinite depletion ($t\rightarrow\infty$) can be related to a simple integral over time-independent scattering solutions

$$\bar{P}_{n\gamma\leftarrow i}(E)=\left|\sum_{\gamma'}\langle\psi_{\gamma'}\bar{F}^{*}_{0\gamma',n\gamma}(E)|\Psi^{0}_{i}\rangle\right|^2 \tag{7}$$

where the total kinetic energy of the fragments exciting in channel ψ_γ is $\varepsilon_{n\gamma}=E+n\hbar\omega-E_\gamma$. This is an extremely useful result. Simply given the time-independent close-coupled solutions, we can always predict the energy distribution of fragments [18]. Of course, this does not tell us how long it takes the initial nonstationary bound state to decay or how long it takes the fragment wave packets to arrive at the detector at $R=\infty$. However, when we construct and evaluate the appropriate wave packets associated with these solutions [19], we obtain a simple expression for the initial-state decay which is related to the Fourier transform of Eq. (7).

In Sec. II we present the time-independent quantal theory of laser-induced scattering using photon number states $|N\rangle$ which are exact energy eigenfunctions of the radiation field. In Sec. III we consider the construction of appropriate wave packets which can represent the photodissociation or photoionization in such a field. In Sec. IV we further modify the wave packet to conform to the coherent radiation state in Eq. (6), and we show what assumptions are required to yield the Floquet ansatz. A specific application of the theory to H_2^+ in Eq. (2) is presented in Sec. V which demonstrates the procedures required, and results that can be obtained from conventional scattering codes. These results are examined in greater detail in the following paper [20] where they are compared to the results obtained from direct integration of the time-dependent Schrödinger equation using a classical field in Eq. (3). (It is perhaps appropriate to mention here that excellent quantitative agreement is obtained between the two methods.) In Sec. VI we consider the photoionization of H in Eq. (1), with specific use of multichannel quantum defect theory (MQDT) to analyze Eq. (7).

II. QUANTAL THEORY OF LASER-INDUCED SCATTERING

We begin our analysis with the conventional channel state expansion of the time-independent scattering wave functions,

$$\Theta_{n\gamma}(N,E,\boldsymbol{\rho},R)=\sum_{n'\gamma'}\theta_{n'\gamma'}(\boldsymbol{\rho})F_{n'\gamma',n\gamma}(N,E,R)\ . \tag{8}$$

These are constructed to be stationary state solutions [17,21] of the combined scattering particles-plus-field Hamiltonian [16]

$$\begin{aligned}H_T&=\hbar\omega(a^{\dagger}a)+H(\mathbf{x},R,\mathbf{A})\\&=\hbar\omega(a^{\dagger}a)+V_{\rm rad}(\mathbf{x},R,\mathbf{A})+T_R+H^0(\mathbf{x},R)\end{aligned} \tag{9}$$

where T_R is the kinetic-energy operator for the radial coordinate R, and the channel state Hamiltonian $H^0=T_{\hat{\mathbf{R}}}+H_{\rm el}(\mathbf{x},R)$ which defines the set of channel states $\psi_{\gamma'}(\mathbf{x})$ in Eq. (5) includes both the radial angular momentum and any remaining internal coordinates of the hydrogen atom in (1) or the diatom in (2) [14]. The classical time-dependent vector potential in Eq. (3) is replaced by the time-independent operator [15–17,21],

$$\mathbf{A}(\mathbf{x})=\frac{c}{\omega}\left[\frac{2\pi\hbar\omega}{V}\right]^{1/2}(a^{\dagger}\hat{\mathbf{e}}e^{i\mathbf{k}_\omega\cdot\mathbf{x}}+a\hat{\mathbf{e}}^{*}e^{-i\mathbf{k}_\omega\cdot\mathbf{x}})\ , \tag{10}$$

and, in the minimal (Coulomb) gauge [22] the radiative interaction is [23]

$$\begin{aligned}V_{\rm rad}(\mathbf{x},R,\mathbf{A})=\sum_i&-(eZ_i/cM_i)\mathbf{p}_i\cdot\mathbf{A}(\mathbf{x}_i)\\&+\frac{(eZ_i/c)^2}{2M_i}\mathbf{A}(\mathbf{x}_i)\cdot\mathbf{A}(\mathbf{x}_i)\ .\end{aligned} \tag{11}$$

The time-independent close-coupled scattering formulation [17,21] is based on defining a product set of particle-plus-field channel states

$$\theta_{n\gamma}(\rho)=|N-n\rangle\psi_\gamma(\mathbf{x}) \tag{12}$$

involving different photon number states $|N\rangle$, $|N\pm1\rangle$, $|N\pm2\rangle\ldots$, which are *energy eigenfunctions* of the quantized source-free radiation field defined by the normal mode functions associated with the frequency ω, polarization $\hat{\mathbf{e}}$, and Poynting vector $\mathbf{k}_\omega$ in Eq. (10). Formally, the particle-field channel states $\theta_{n\gamma}(\rho)$ now span the combined space $\rho=(q_\omega,\mathbf{x})$ where $q_\omega=(\hbar/2\omega)^{1/2}(a+a^{\dagger})$ [which implies $\dot{q}_\omega=-i(\hbar\omega/2)^{1/2}(a-a^{\dagger})$] is a generalized position "coordinate" for the single laser mode. This construction yields

$$\left[\hbar\omega a^{\dagger}a - i\hbar\frac{\partial}{\partial t}\right]e^{-iN\omega t}|N\rangle = 0 ,$$

and ensures that, asymptotically, the channels are exact eigenfunctions of $H_T(R=\infty)$ as they must be to satisfy the requirements of scattering theory [24],

$$\lim_{R\to\infty}(H_T - E_T)\theta_{n\gamma}(\rho)e^{\pm ik_{n\gamma}R}/R = 0 . \tag{13}$$

The combined particle-plus-field energy $E_T = E + N\hbar\omega$ is a constant of the emotion, and, for a given initial number state $|N\rangle$, the energy E is conserved. This can be used to define the asymptotic kinetic energy in each channel [23],

$$\begin{aligned}\varepsilon_{n\gamma} &= (\hbar k_{n\gamma})^2/2M = E_T - [E_\gamma + (N-n)\hbar\omega] \\ &= E - E_\gamma + n\hbar\omega\end{aligned} \tag{14}$$

where E_γ, defined asymptotically by $\lim_{R\to\infty}H^0\psi_\gamma = E_\gamma\psi_\gamma$, represents the sum of the internal energies and M the reduced mass of the scattered fragments associated with the channel state ψ_γ. The index n, which is associated with the number state $|N-n\rangle$, represents the number of photons that have been removed by absorption ($n>0$) from the initial number state $|N\rangle$ or added to it by stimulated emission ($n<0$).

If we restrict the expansion in Eq. (8) to include only a finite number N_T of particle-field channel states the matrix of coupled radial equations generated by the Schrödinger equation, $(H_T - E - \hbar\omega N)\Theta_{n\gamma} = 0$, i.e.,

$$\begin{aligned}&[T_R + \mathbf{U}(N,R) - E]\mathbf{F}(N,E,R) = 0 , \\ &U_{n'\gamma',n\gamma}(N,R) = \langle\theta_{n'\gamma'}|V_{\text{rad}}|\theta_{n\gamma}\rangle \\ &\qquad + \delta_{n',n}(\langle\theta_{n\gamma'}|H^0|\theta_{n\gamma}\rangle - n\hbar\omega)\end{aligned} \tag{15}$$

can be solved using the usual close-coupling procedures. Let us arrange the channel indices $\{n\gamma\}$ in order of increasing asymptotic energy. Generally the set of $N_T = N_0 + N_C$ channels $\{n\gamma\}$ contains a subset of N_0 open channels with $\varepsilon_{n\gamma} > 0$ and N_C closed channels with $\varepsilon_{n\gamma} < 0$ which we further designate as $\{o\}$ and $\{c\}$, respectively. At a given energy E_T we obtain an N_0-fold degenerate set of orthogonal energy-normalized solution vectors, by imposing the following asymptotic behavior on the radial wave functions:

$$\begin{aligned}&F_{c',o} \underset{R\to\infty}{\sim} 0 , \\ &F_{o',o} \underset{R\to\infty}{\sim} \left[\frac{2\mu}{\pi k_{o'}\hbar}2\right]^{1/2} \\ &\qquad \times [e^{-ik_oR}\delta_{o',o} - e^{+ik_{o'}R}S_{o',o}(N,E)]/2iR\end{aligned} \tag{16}$$

where $\mathbf{S}$ is the $N_0 \times N_0$ unitary scattering matrix.

For a given incident channel state $\theta_{n\gamma} = |N-n\rangle\psi_\gamma$ we expect that a possibly large but finite range $|n'-n| = 0,1,2,\ldots$ of final channel states $\theta_{n'\gamma'} = |N-n'\rangle\psi_{\gamma'}$ will contribute to the solution vector $F_{n'\gamma',n\gamma}(N,E,R)$ centered about $n'=n$. Thus even for modestly intense laser fields we can assume $N \gg |n'|, |n|$ such that

$$\frac{dF_{n'\gamma',n\gamma}(N,E,R)}{dN} \approx 0 \text{ and } \frac{dS_{n'\gamma',n\gamma}(N,E)}{dN} \approx 0 \quad \text{if } N \gg |n'|, |n| . \tag{17}$$

As we shall see in Sec. IV, this will be a sufficient condition to derive the Floquet expressions (4) and (5).

The time-independent wave function $\Theta_{n\gamma}(N,E)$ in Eq. (8) corresponds to an "incoming" state prepared in the *incident* channel $|N-n\rangle\psi_\gamma$ with total energy $E_T = E + N\hbar\omega$. Implicitly one assumes that the "initial" state in a given experiment is represented by an incoming wave packet at $t\to-\infty$ that is sufficiently extended in time to allow arbitrarily precise evaluation of the total collision energy $E_T = E + N\hbar\omega$. Such a wave packet is well approximated as a pure eigenstate of the total energy,

$$\Omega^{+}_{n\gamma}(N,E,\mathbf{x},R,t) = \Theta_{n\gamma}(N,E,\boldsymbol{\rho},R)e^{-iEt/\hbar}e^{-iN\omega t} , \tag{18a}$$

for the incoming state. A comparable "outgoing" wave packet which we designate as

$$\Omega^{-}_{n\gamma}(N,E,\mathbf{x},R,t) = \Theta^{*}_{n\gamma}(N,E,\boldsymbol{\rho},R)e^{-iEt/\hbar}e^{-iN\omega t} , \tag{18b}$$

for the outgoing state, is obtained by replacing $\Theta_{n\gamma}$ with the conjugate function $\Theta^{*}_{n\gamma}$. These are only approximations to a real experimental situation since the field described by pure number states $|N\rangle$ can differ substantially from the typically classical optical cavity mode [16]. In Sec. IV we will use this complete set of number state scattering wave functions to construct more realistic wave packets for scattering by a laser in a pure time-dependent coherent state $|\bar{\alpha}(t)\rangle$.

III. HALF-COLLISION ANALYSIS OF LASER-INDUCED DECAY OF BOUND STATES

Before proceeding to the coherent-state wave packet, we will consider the proper use of these full-collision wave functions to describe a half-collision process corresponding to the photodissociation (photoionization) of some initial bound state $\Phi_i(N,\boldsymbol{\rho},R)$,

$$\Phi_i(N,\boldsymbol{\rho},R) \equiv \sum_{c'=n'\gamma'}\theta_{c'}(\boldsymbol{\rho})\mathcal{P}_{c',i}(N,E_i,R) , \tag{19a}$$

which is subject to a laser incident in a pure number state $|N\rangle$ at $t=0$. Radiative interactions cause the state to become *nonstationary* and it subsequently decays into the complete set of outgoing states defined by Eq. (18b). We have expanded this state in the same complete set of *closed*-channel states $\{c'\}$ used in (8), but the radial functions $\mathcal{P}_{c',i}(N,E_i,R)$ are *not* solutions to Eq. (15), since Φ_i represents a solution to some totally different Hamiltonian which describes conditions just *before* the field was introduced and generally excludes the set of open channels $\{o\}$. The expansion (19a) includes channels $c'=(n'\gamma')$ with $n'\neq 0$ and can allow for initial dressing of the bound

state by the applied field. However, in many experiments we expect that Φ_i is best represented as a field-free bound state associated with a specific closed channel $c=(0\gamma)$ and a radial function in the bound state i,

$$\Phi_i(N,\boldsymbol{\rho},R)\approx\theta_c(\boldsymbol{\rho})\mathcal{P}_{c,i}(R)\equiv|N\rangle\Psi_i^0(\mathbf{x},R) \tag{19b}$$

where $\Psi_i^0=\psi_\gamma(\mathbf{x})\mathcal{P}_{c,i}(R)$ and $E_i^0=E_i-N\hbar\omega$ approximate the initial field-free particle state and its energy. The radial function $\mathcal{P}_{c,i}(R)$ represents a specific normalized bound state i supported in the *field-free* attractive diagonal potential $U_{cc}(R)=\langle c|H^0|c\rangle$

$$[T_R+U_{c,c}(R)-E_i^0]\mathcal{P}_{c,i}(R)=0 \tag{20}$$

and can be viewed as a resonance state in the closed channel c. It should be emphasized that this initial state is predicated on a particular experimental situation where the initial bound state is an exact eigenfunction of the *field-free* (T_r+H^0) which is "abruptly" exposed to the laser field at $t=0$ [26]. Specific examples are given in Secs. V and VI.

We can always use the *complete* set of *outgoing* number state solutions (18b) to form an appropriate nonstationary wave packet [18,19]

$$\Omega_i(N,\boldsymbol{\rho},R,t)=\sum_{o=n\gamma}\int dE\,\Omega_{n\gamma}^-(N,E,\boldsymbol{\rho},R,t)C_{n\gamma\leftarrow i}(N,E)$$
$$\underset{t\to 0}{\sim}\Phi_i(N,\boldsymbol{\rho},R) \tag{21}$$

where the channel summation is restricted to the set of open channels $\{o\}$. The coefficients $C_{n\gamma\leftarrow i}$ are given by the following expressions using Eqs. (16) and (19a):

$$C_{o\leftarrow i}(N,E)=\langle\Theta_o^*(N,E)|\Phi_i(N)\rangle$$
$$=\sum_{c'}\langle F_{c',o}^*(N,E)|\mathcal{P}_{c',i}\rangle\ , \tag{22a}$$

or (19b)

$$C_{o\leftarrow i}(N,E)=\langle F_{c,o}^*(N,E)|\mathcal{P}_{c,i}\rangle\ , \tag{22b}$$

respectively. In Sec. V the coefficient $C_{o\leftarrow i}(n,E)$ is evaluated numerically [28] using the matrix $\mathbf{F}(N,E,R)$ of close-coupled radial solution vectors for H_2^+ MPD, while in Sec. VI MQDT is used [2] to obtain (22) from the close-coupled solutions for H atom MPI.

All the subsequent dynamics of this *abruptly* prepared initial bound state can be extracted from the wave packet (21). For instance, the probability of finding the system in the outgoing dissociated state $\Omega_{n\gamma}^-(N,E,t)$, which is an exact eigenstate of the total Hamiltonian H_T, is *independent* of time [29] and simply given by the expansion coefficient in Eq. (22),

$$P_{n\gamma\leftarrow i}(N,E)=|\langle\Omega_{n\gamma}^-(N,E,t)|\Omega_i(N,t)\rangle|^2$$
$$\equiv|C_{n\gamma\leftarrow i}(N,E)|^2\ . \tag{23}$$

This defines the probability that fragments originating from the particle channel state ψ_γ with total internal energy E_γ are produced via an n-photon absorption with relative kinetic energy $\varepsilon_{n\gamma}$ given by Eq. (14). The total probability of dissociation or ionization in the infinite depletion limit must sum to unity:

$$\sum_{n,\gamma}\int dE\,P_{n\gamma\leftarrow i}(N,E)=\sum_{n,\gamma}b_{n\gamma\leftarrow i}(N)=1\ . \tag{24}$$

The sum only extends over open channels and $b_{n\gamma\leftarrow i}(N)$ defines an integrated branching ratio into the energetically accessible channel $\theta_{n\gamma}$.

The probability of this nonstationary wave packet remaining in the initial state at times $t>0$ is simply given as follows:

$$P_i(N,t)=|\langle\Phi_i(N)\exp(-iE_it/\hbar)|\Omega_i(N,t)\rangle|^2$$
$$\equiv\left|\int dE\left[\sum_{n,\gamma}P_{n\gamma\leftarrow i}(N,E)\right]e^{-i(E-E_i^o)t/\hbar}\right|^2\ . \tag{25}$$

In many circumstances we find that $P_{n\gamma\leftarrow i}(N,E)$ is well represented to high order by a perfect Lorentzian expression

$$P_{n\gamma\leftarrow i}(N,E)\approx b_{n\gamma\leftarrow i}(\Gamma_i/2\pi)/[(E-E_i^{\rm ac})^2+(\Gamma_i/2)^2] \tag{26}$$

where the initial bound-state energy $E_i^{\rm ac}=E_i+\Delta_i$ is basically ac Stark "shifted" by an amount Δ_i due to multiphoton interactions, and we can extract a total laser-induced rate "constant" $\Gamma_i/\hbar$ for the decay of the initial state $\Phi_i=|N\rangle\Psi_i^0$ from this expression. Whenever this Lorentzian behavior can be confirmed far in the wings of Eq. (26) we can avoid the explicit numerical evaluation of Eq. (25) and simply infer a near-perfect exponential decay of the initial bound state

$$P_i(N,t)\approx\exp(-\Gamma_it/\hbar)\ . \tag{27}$$

IV. COHERENT-STATE WAVE PACKETS AND FLOQUET THEORY

The Floquet wave functions (4) and (5) represent an interaction picture wave packet, which treats the time-dependent radiation field classically. In this paper we want to emphasize the equivalence of using a fully quantal description of the half-collision process in the strong laser field limit. Note that the set of time-independent close-coupled equations which define the Floquet radial solution vectors $\bar{\mathbf{F}}(E,R)$ in Eq. (5) are *identical* to the set of Eqs. (15) which define the fully quantal radial solution vectors $\mathbf{F}(\bar{N},E,R)$ in Eq. (15), with N simply replaced by the effective photon number $\bar{N}$ associated with the classical field in Eq (3). Using the time-independent Schrödinger representation of the radiation field we will arrive at a result identical to Eq. (5), with $\bar{\mathbf{F}}(E,R)\equiv\mathbf{F}(\bar{N},E,R)$, but hopefully with a better and more unified interpretation of the initial preparation and subsequent evolution of *observable* properties associated with this wave packet.

We shall only be considering fields for which $N\gg1$ and we can safely dispense with the zero point energy in the laser mode. As is well known [16] the quantum-mechanical number state $|N\rangle$, which precisely specifies the total energy $N\hbar\omega$ of the eigenmode, yields complete uncertainty in the phase ϕ of the field in Eq. (3) such that the expectation value for the electric field vanishes,

$\langle N|\mathbf{E}|N\rangle=0$, and only $\langle N|\mathbf{E}\cdot\mathbf{E}|N\rangle=\hbar\omega(4\pi N/V)$ has a classical analog. We shall use the complete set of exact time-independent number state solutions $\Theta_{n\gamma}(N,E,\boldsymbol{\rho},R)$ to construct a particle-plus-field wave packet incident in the pure *coherent* state $|\bar{\alpha}(t)\rangle$ given in Eq. (6). This is the quantum equivalent of the classically stable field (3) and gives the minimum uncertainty in the field parameters. The function $|\bar{\alpha}\rangle$ is an exact eigenfunction of the annihilation operator

$$a|\bar{\alpha}\rangle=\bar{\alpha}|\bar{\alpha}\rangle=e^{-i\phi}\sqrt{\bar{N}}\,|\bar{\alpha}\rangle \tag{28}$$

such that $\langle\bar{\alpha}|a^{\dagger}a|\bar{\alpha}\rangle=\bar{N}$ and

$$\langle\bar{\alpha}|\mathbf{E}(t)|\bar{\alpha}\rangle=-(8\pi\bar{N}\hbar\omega/V)^{1/2}\hat{\mathbf{e}}\sin(\omega t-\mathbf{k}_{\omega}\cdot\mathbf{x}+\phi)\ . \tag{29}$$

In principle, explicit laser pulse shapes can be described by introducing a time dependence into the coherent-state eigenvalues $\bar{\alpha}(t)=e^{-i\phi(t)}\sqrt{\bar{N}(t)}$. In practice, it is numerically much more efficient to simply integrate the time-dependent Schrödinger equation [3,8] using the classical field (3) with time-dependent amplitudes $\bar{\mathbf{E}}(t)$ and or phase $\phi(t)$.

In place of the number state wave packet in Eq. (18), we can weight the infinite set of such incident scattering states with the normalized set of Gaussian coefficients defined in Eq. (6) [15]. This defines a new wave packet which is still incident in the particle channel state ψ_{γ}, but which now scatters in the presence of a coherent laser mode $|\bar{\alpha}\rangle$.

$$\begin{aligned}\bar{\Omega}^{+}_{n\gamma}(E,t)&=\sum_{N}\bar{c}(N)\Omega^{+}_{n\gamma}(N,E,t)\\&=\sum_{N}\bar{c}(N)e^{-iN\omega t}\Theta_{n\gamma}(N,E)e^{-iEt/\hbar}\\&=\sum_{n'}\left[\sum_{N}\bar{c}(N)e^{-iN\omega t}|N-n'\rangle\right]\\&\quad\times\sum_{\gamma'}\psi_{\gamma'}F_{n'\gamma',n\gamma}(N,E)e^{-iEt/\hbar}\end{aligned} \tag{30}$$

where $\bar{c}(N)=e^{-|\bar{\alpha}|^2/2}(\bar{\alpha})^N/\sqrt{N!}$. The peaked value $|\bar{N}\rangle$ in the Poisson distribution of number states in (6) is determined by equating $(8\pi\bar{N}\hbar\omega/V)^{1/2}\hat{\mathbf{e}}$ in Eq. (29) to $\bar{\mathbf{E}}$ in the classical expression for $\mathbf{A}$ in (3). The fractional uncertainty $|\Delta|/\bar{N}$ in the distribution of number states $|\bar{N}-\Delta\rangle$ about the mean value $\bar{N}$ decreases as $1/\sqrt{\bar{N}}$ and we can use Eq. (17) to justify replacing $\mathbf{F}(N,E)$ by the mean value solution vectors $\mathbf{F}(\bar{N},E)$ in Eq. (30). We are now free to replace the summation index N within the brackets by $M=N-n'$. Noting that, for $N\gg n'$

$$\bar{c}(N)/\bar{c}(N-n')=\frac{(\bar{\alpha})^{n'}[(N-n')!]^{1/2}}{\sqrt{N!}}\rightarrow e^{-in'\phi} \tag{31}$$

we can sum the bracketed term

$$\left[\sum_{N}\bar{c}(N)e^{-iN\omega t}|N-n'\rangle\right]\rightarrow|\bar{\alpha}(t)\rangle e^{-in'(\omega t+\phi)} \tag{32}$$

and express the quantal wave packet (30) as follows:

$$\bar{\Omega}^{+}_{n\gamma}(E,t)=|\bar{\alpha}(t)\rangle\left[\sum_{n'}\sum_{\gamma'}\psi_{\gamma'}F_{n'\gamma',n\gamma}(\bar{N},E)\times e^{-in'(\omega t+\phi)}\right]e^{-iEt/\hbar} \tag{33}$$

$$=|\bar{\alpha}(t)\rangle\bar{\Psi}^{+}_{n\gamma}(E,t)\ . \tag{34}$$

Thus, in the limit of strong fields, the fully quantal wave packet factors into a product of a *coherent state which remains unperturbed* by the laser-induced particle interactions, and a time-dependent Floquet-like scattering wave function that conforms to the classical interaction picture with $\mathbf{F}(\bar{N},E,R)$ equivalent to $\bar{\mathbf{F}}(E,R)$ in Eq. (5). Note that for a given mean $\bar{N}$ the set of incoming Floquet states $\bar{\Psi}^{+}_{n\gamma}(E,\mathbf{x},R,t)$, when averaged over an optical cycle $\tau=2\pi/\omega$, form a complete "energy" normalized orthonormal set

$$(1/\tau)\int_{0}^{\tau}dt\,\langle\bar{\Psi}^{+}_{n'\gamma'}(E',t)|\bar{\Psi}^{+}_{n\gamma}(E,t)\rangle=\delta_{n',n}\delta_{\gamma',\gamma}\delta(E'-E)\ . \tag{35}$$

A comparable complete set of outgoing Floquet states $\bar{\Psi}^{-}_{n\gamma}(E,t)$ is obtained by replacing $\mathbf{F}(\bar{N},E,R)$ with its conjugate in Eqs. (5) and (33).

We can perform the same coherent-state summation on Eq. (21) to construct a nonstationary wave packet $\bar{\Omega}_i(\boldsymbol{\rho},R,t)\underset{t\rightarrow 0}{\sim}|\bar{\alpha}(0)\rangle\Psi^{0}_{i}(\mathbf{x},R)$ which represents exposing a system in the initial bound state Ψ^{0}_{i} to a coherent radiation field $|\bar{\alpha}\rangle$ at $t=0$, rather that to the number state $|N\rangle$ in Eq. (19b),

$$\begin{aligned}\bar{\Omega}_i(t)&=\sum_{N}\bar{c}(N)\Omega_i(N,E,t)\\&=\sum_{N}\bar{c}(N)\sum_{n}\sum_{\gamma}\int dE\,\Omega^{-}_{n\gamma}(N,E,t)C_{n\gamma\leftarrow i}(N,E)\\&\approx|\bar{\alpha}(t)\rangle\sum_{n}\sum_{\gamma}\int dE\,\bar{\Psi}^{-}_{n\gamma}(E,t)C_{n\gamma\leftarrow i}(\bar{N},E)\\&\equiv|\bar{\alpha}(t)\rangle\bar{\Psi}_i(\bar{E}_i,\mathbf{x},R,t)\end{aligned} \tag{36}$$

where we have utilized Eq. (17) to justify replacing $C(N,E)$ with his mean value $C(\bar{N},E)$ in (36). The half-collision Floquet state in Eq. (4) is an approximation to the following expression:

$$\begin{aligned}\bar{\Psi}_i(\bar{E}_i,\mathbf{x},R,t)&\equiv\sum_{n}\sum_{\gamma}\int dE\,\bar{\Psi}^{-}_{n\gamma}(E,\mathbf{x},R,t)C_{n\gamma\leftarrow i}(\bar{N},E)\\&\underset{t\rightarrow 0}{\sim}|\bar{\alpha}(0)\rangle\Psi^{o}_{i}(\mathbf{x},R)\ .\end{aligned} \tag{37}$$

If we use Eq. (35) and average the absolute square of the projection of the outgoing Floquet states onto this bound-state wave packet over one optical cycle, we obtain the same expressions for the distribution of dissociated states as given in Eq. (23) with $N\equiv\bar{N}$.

$$\bar{P}_{n\gamma\leftarrow i}(E)\approx P_{n\gamma\leftarrow i}(\bar{N},E)\ . \tag{38}$$

The amplitude for the wave packet (36) remaining in the initial state $|\bar{\alpha}(t)\rangle\Psi^{0}_{i}e^{-iE^{0}_{i}t/\hbar}$ is given by the projection

$$\langle \bar{\alpha}|\langle \Psi_i^0 e^{-iE_i^0 t/\hbar}|\bar{\Omega}_i\rangle = \sum_M \sum_N \bar{c}(N)\bar{c}(M)^* \int dE \sum_{n,\gamma} e^{i(M-N)\omega t}\langle M|\langle \Psi_i^0|\Theta^*_{n\gamma}(N,E)\rangle C_{n\gamma\leftarrow i}(N,E) e^{i(E_i^0-E)t/\hbar}.$$

Again averaging the absolute square of this amplitude over one optical cycle, we obtain the following probability of the wave packet remaining in the initial state:

$$\bar{P}_i(t) = |\langle \bar{\alpha}|\langle \Psi_i^0 e^{-iE_i^0 t/\hbar}|\bar{\Omega}_i\rangle|^2 = \left| \sum_N |\bar{c}(N)|^2 \int dE \sum_{n,\gamma} C^*_{n\gamma\leftarrow i}(N,E) C_{n\gamma\leftarrow i}(N,E) \times e^{i(E_i^0-E)t/\hbar} \right|^2 . \quad (39)$$

Using Eq. (17) to justify replacing $C(N,E)$ with $C(\bar{N},E)$ and noting that the coherent-state coefficients $\bar{c}(N)$ are normalized to one, we obtain

$$\bar{P}_i(t) \approx \left| \int dE \left[\sum_{n,\gamma} P_{n\gamma\leftarrow i}(\bar{N},E) \right] e^{i(E_i^0-E)t/\hbar} \right|^2 . \quad (40)$$

This final result is simply equivalent to Eq. (25) with N replaced by $\bar{N}$.

We have arrived at the rather simple and anticipated result that we can often represent laser-induced phenomena in intense fields simply by using a single number state $|\bar{N}\rangle$ to represent the more proper coherent states $|\bar{\alpha}\rangle$. This can be attributed to the factorization of the wave functions in Eq. (33) and (36) in the strong field limit, which implies that the radiative field simply acts as an infinite reservoir (or sink) of photons. Obviously, this means we can only calculate observable properties associated with the scattered particles. We now consider the application of these simple results to processes (1) and (2).

V. DISCUSSION OF RESULTS FOR H_2^+ AND MPD

In studying the strong field dissociation of H_2^+ we [30] expand the full-collision wave function in Eq. (8) over the restricted set of molecule-field channel states $\theta_{n\gamma} \equiv |N-n\rangle\psi_\gamma$ where $\gamma=(\Lambda,J,M)$ only includes the two lowest electronic states $\Lambda \equiv 1s\sigma_g(^2\Sigma_g^+)$ and $2p\sigma_g(^2\Sigma_u^+)$ which correlate with the fragments $H^+ + H(1s)$. The quantum numbers J and M designate the total angular momentum of the field-free molecule.

Because the two radiatively coupled Λ states are asymptotically degenerate for H_2^+ the radiative interaction in the dipole approximation, using the usual electric field (EF) [22] or "length" gauge [31], becomes infinitely divergent as the internuclear coordinate $R \to \infty$. Bates [32] evaluated the transition moment $\mu^{EF}(R)$ for the $1s\sigma_g \to 2p\sigma_u$ transition in H_2^+ and found it diverges as $R/2$. By evaluating the radiative interactions in the radiative field (RF) or velocity gauge we avoid this divergence [30]. This had already been noted by Chakrabarti, Bhattacharyya, and Saha [33] for HD^+, who recommend using the convergent radiative gauge (RF) whenever free-free molecular transitions are involved (see Refs. [2] and [5] for discussions of similar divergences in electron-ion scattering). Numerical values for the RF (velocity) dipole transition moment $\mu^{RF}(R)$ are deduced from the EF (length) results of Bates by using the commutator relation $\langle u|\mathbf{A}\cdot\mathbf{p}|g\rangle = [\Delta U(R)/h\nu]\langle u|\mathbf{E}\cdot\mathbf{x}|g\rangle/c$, where $\Delta U(R) = U_u - U_g$ is the energy difference between the two states u and g which are asymptotically degenerate [34]. This device permits us to use a truncated set of channel states and still apply physically meaningful scattering boundary [24] conditions to our close-coupled radial solutions in Eqs. (15) and (16). Unfortunately, since only two electronic states of H_2^+ are employed in these calculations there is no assurance that gauge invariance [35] will be satisfied. In fact, based on as yet unpublished calculations of Muller [36] it would appear that any ultimately converged results will be much more in keeping with the two-state length gauge calculations first proposed by Zavriyev *et al.* [37] rather than the present two-state velocity gauge model. However, for the general purpose of demonstrating the wave-packet description for laser-induced half-collision processes we shall continue to employ the velocity gauge model.

At each interatomic distance R, only molecule-field channel states whose occupation numbers differ by one photon can be directly coupled by the RF radiative interactions. (Actually the $\mathbf{A}\cdot\mathbf{A}$ operator can introduce $|n-n'|=2$ couplings [25] which are generally ignored.) In the weak field limit, these couplings correspond to typically allowed, one-photon electronic-rotational transitions $\Lambda,J,M \to \Lambda',J',M'$ which are well described by perturbation theory and conform to the usual molecular selection rules. However, in the strong field limit, the radial motion associated with the photodissociation of an initially bound vibrational level of the molecule is best solved in full multichannel close coupling without any recourse to perturbation theory.

Results have already been presented in Ref. [30] for photodissociation of the $v=0$ state of $H_2^+(1s\sigma_g\,^2\Sigma_g^+)$ by $\lambda=3297$ Å radiation for a range of intensities $I=7.0\times10^{12}-5.6\times10^{13}$ W/cm^2. A "mean" J value was used which implies that the effect of optical pumping of the rotational levels was ignored [38], and the molecule was considered aligned by the linearly polarized field. Projecting the outgoing multichannel scattering wave functions onto the initial bound state in Eq. (22) we obtain the line shapes (23) and decay behavior (25). Although we have not made any commitment to an exponential decay of the initial state, as is implicitly inferred in the usual complex-quasienergy approach [39] to the half-collision Floquet ansatz, the Lorentzian behavior (26) and exponential decay (27) is well substantiated by our numerical results. An example of one such line shape is shown in Fig. 1. In this case the total width and resultant decay rate agree perfectly with the complex eigenvalue approach used in Ref. [9]. In addition, Eq. (23) gives us the probability that the fragments possess a kinetic energy associated with an n-photon dissociation process.

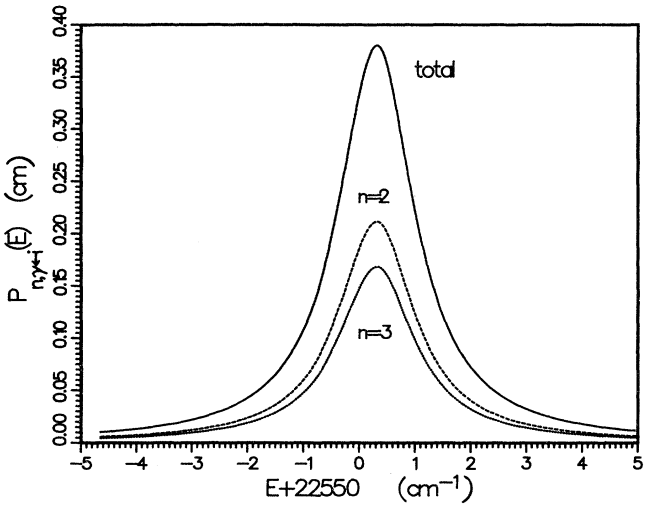

FIG. 1. Energy distribution of $H(1s)+H^+$ photofragments from $H_2^+(\sigma_g,v=0)$ for $\lambda=329.7$ nm and intensity $I=1.4\times10^{13}$ W/cm^2. The relative kinetic energy ε_n of the fragments formed by absorption of n photons is $\varepsilon_n=E+n\hbar\omega$. The total probability distribution $\sum_n P_{n\gamma\leftarrow i}(E)$, as well as each of the individual n-photon peaks, are almost perfectly Lorentzian with a half-width $\Gamma_i=1.7$ cm^{-1} which predicts a pure exponential decay of the initial state, with a dissociation rate 3.2×10^{11} s^{-1}.

Note that, although the rate of decay was primarily third order in I, the separating fragments returned one photon to the field by stimulated emission, and the observed distribution of fragments conformed to $n\approx2$.

Another example is shown in Fig. 2(a), with $\lambda=2480$ Å and $I=2\times10^{+14}$ W/cm^2. Here we obtain a distinctly non-Lorentzian line shape for the photodissociation from $v=2$. As emphasized in Ref. [30] the exact close-coupled scattering wave functions $\mathbf{F}(\bar{N},E,R)$ which enter Eq. (22) and define the line shape in Eqs. (23) and (38) are very well understood in terms of the "adiabatic" molecule-field dressed-state potentials obtained by diagonalizing the "diabatic" interaction matrix $\mathbf{U}(N,R)$ in Eq. (15). The dashed curves in Fig. (3) show the resultant adiabatic potentials defined by the parameters associated with Fig. 2(a). Starting with an initial wave packet with a vibrational wave function $\mathcal{P}_{c,i}(R)$ in Eq. (22b) defined by the diabatic $\Lambda=\sigma_g(v=2)$ state, which has an eigenvalue $E_2=-16\,949$ cm^{-1} in the absence of the laser field, this is primarily projected onto a resonance state defined by the adiabatic potential at $E_2\approx-27\,300$ cm^{-1} which is, of course, substantially broadened by what can be viewed as a multiphoton laser-induced "predissociation." This shows up as the major peak in Fig. 2(a). However, we see that there is also a significant component projected onto the adiabatic $v=1$ state at $E_1\approx-28\,825$ cm^{-1} as well as other structure in $P_{n\gamma\leftarrow i}$ which might be attributed to a very small adiabatic $v=0$ and a significant adiabatic $v\approx3$ contribution to Fig. 2(a).

The line shapes are defined in the infinite depletion limit. The total decay of the initial $v=2$, $\Lambda=^2\Sigma_g^+$ population as a function of time is simply obtained by performing the Fourier transform over the total line shape in Eq.

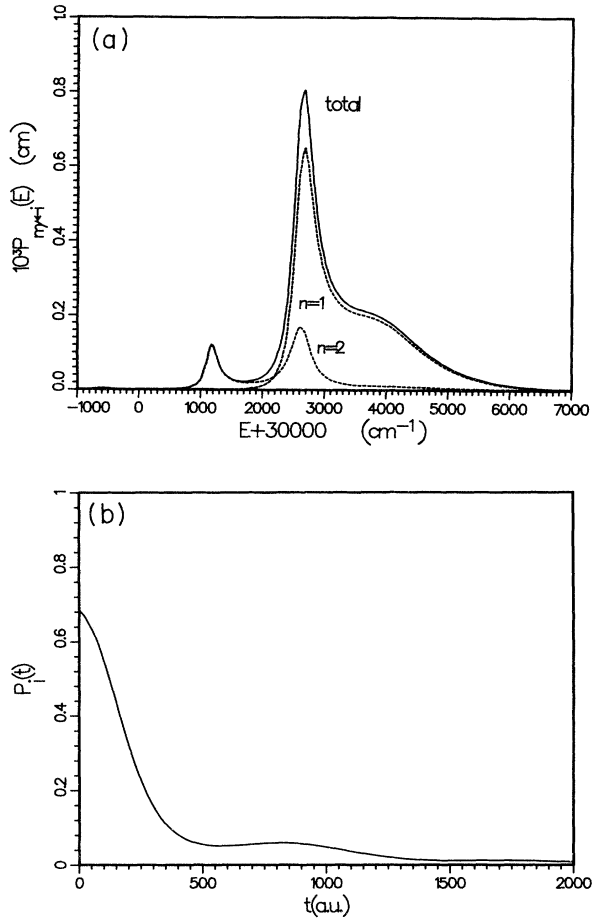

FIG. 2. (a) Probability distribution per unit energy of photofragments from $H_2^+(\sigma_g,v=2)$ for $\lambda=248.0$ nm and intensity $I=2.0\times10^{14}$ W/cm^2. Only 0.82 of the fragment distribution is contained in this energy region, and the remaining 0.18 is distributed over broad range of energies. (b) The probability of the half-collision wave packet remaining in the initial state exhibits distinctly nonexponential decay. The initial value 0.67 of the population at $t\approx0$ represents the rapid depletion of the population which yields the fragments not contained in (a).

(40), and results in the very nonexponential time dependence shown in Fig. 2(b). For instance, the dip in the decay curve at $t\approx550$ a.u. can be associated with the "destructive" interference of the adiabatic $v=1$ and 2 contributions to Eq. (40) when $(E_2-E_1)t/\hbar\approx\pi$. It is interesting to note the different line shapes for branching into the $n=1$ and 2 channels in Fig. 2(a), which implies different histories of formation due to such interference effects. Further details of the nonexponential decay are analyzed in the following paper [20]. In particular we must note that the total line shape in Fig. 2(a) only integrates to about 0.82. This appears squared in Eq. (40) and thus the initial-state population in Fig. 2(b) is already depleted by 67% at $t\approx0$. Actually the remaining 0.18 contribution to the line shape is distributed over a very broad distribution of "continuum" energies which would indicate an almost instantaneous 33% depletion of the initial popula-

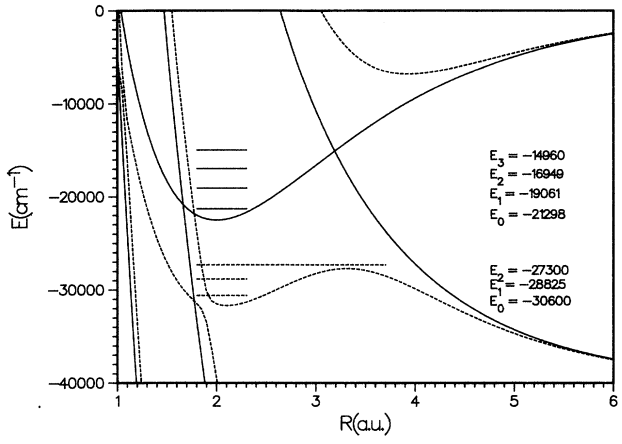

FIG. 3. Diabatic (solid) and adiabatic (dashed) field-dressed potentials for H_2^+ with $\lambda=248.0$ nm and $I=2.0\times10^{14}$ W/cm^2. The attractive diabatic curve represents the $1s\sigma_g$ state associated with the number state $|\bar{N}-n\rangle$ with $n=0$. This undergoes a diabatic crossing at $R\approx3.3$ a.u. with the repulsive $2p\sigma_u$ diabatic state and number state $|\bar{N}-n\rangle$ with $n=1$. The stable diabatic vibrational bound states are located by solid lines in the diabatic $1s\sigma_g$ potential. The approximate bound states in the adiabatic potential which asymptotically correlate with $n=1$ are shown by dashed lines. These appear as broadened peaks in the kinetic-energy distribution in Fig. 2(a).

tion at the onset of the laser pulse. In the following paper [20] we will tediously account for all the missing population by performing the integration (40) over a broad range of E. Doing this we will find quantitative agreement with the results obtained from direct integration of the time-dependent Schrödinger equation using the classic field in Eq. (3), *and averaging over the initial phase* ϕ. This is the classical equivalent to the requirement in the present derivation of the Floquet-type theory of averaging over an optical cycle to obtain Eqs. (38) and (40). Although we are able to show the equivalence of the two approaches, realistically, such rapidly decaying components are basically incompatible with our assumption that we can average our "observations" over an optical cycle. Such "transient" behavior is best left to the exact integration of the time-dependent Schrödinger equation [20] using realistic pulse shapes to describe particular experiments of interest.

VI. MCQDT ANALYSIS OF MPI FOR HYDROGEN

Dimou and Faisal [13] first utilized the full-collision ansatz (5) to analyze the laser-induced resonance structure for $e+H^+$ scattering. A general MQDT analysis of the closed-channel contributions to such a scattering wave function was then introduced by Giusti-Suzor and Zoller [2] to predict the above-threshold-ionization rates for the associated *half*-collision process originating from the high Rydberg levels of H. The initial Rydberg levels can be viewed as undergoing a laser-induced autoionization. Although not explicitly stated, the MQDT analysis implies the construction of a decaying wave packet comparable to (37). Actually, a Lorentzian-like behavior of the initial nonstationary (autoionizing) bound state was observed in the low-intensity calculations, and greatly facilitates extracting the photoionization rates and branching ratios. However, we wish to emphasize that the MQDT analysis introduced in Ref. [2] is not committed to the perturbative approximations inherent in the complex-quasienergy approach that is often applied to Eq. (4) [1,5,9,11], and it can reliably calculate the nonexponential behavior associated with strongly broadened overlapping resonances. For a thorough study of Rydberg wave packets generated by laser pulses, the reader is referred to the review by Alber and Zoller [40].

Starting from the Floquet ansatz for the *full*-collision process of $e+H^+$ in a strong laser field, the radiative close-coupling equations have been solved [2] in the "space-translation frame." This amounts to choosing the acceleration form for the dipolar interaction and ensures rapid convergence of the radiative couplings with increasing radial distance. The reaction matrix thus obtained varies slowly with the asymptotic energy of the electron, and can be extrapolated across the ionization threshold. Thus a single close-coupling calculation performed slightly above threshold was sufficient to allow a MQDT analysis of the closed-channel resonances associated with highly excited Rydberg states of the atom. These states are perfectly stationary in the absence of the field, and are subject to laser-induced autoionization once the field is present.

Using the notations of Sec. II, we can block the $N_T\times N_T$ matrix of radial solution vectors in Eq. (15) (and all other such matrices) as follows:

$$\mathbf{F}(\mathbf{S};N,E,R)=\begin{bmatrix}\mathbf{F}_{00}(\mathbf{S}) & \mathbf{F}_{0C}(\mathbf{S})\\ \mathbf{F}_{C0}(\mathbf{S}) & \mathbf{F}_{CC}(\mathbf{S})\end{bmatrix} \tag{41}$$

$\mathbf{F}(\mathbf{S})$ designates the particular set of solution vectors which satisfy the incoming scattering boundary conditions associated with the unitary $N_0\times N_0$ scattering matrix $\mathbf{S}$ in Eq. (16). Only the first N_0 solution vectors are proper (normalizable) wave functions, while the asymptotically divergent terms have been segregated in the remaining N_C vectors and are rejected as unphysical.

The beauty of MQDT is that we can solve the coupled equations at some total energy $E_T=E+N\hbar\omega$ just above the ionization threshold when *all* channels are open, i.e., $\varepsilon_{n\gamma}>0$ in Eq. (14), and extract a real symmetric $N_T\times N_T$ matrix $\mathbf{Y}(N,E)$ which is an analytic and *slowly varying* function of E and completely summarizes all the close-coupled dynamics between the channel states.

$$\mathbf{F}(\mathbf{Y};N,E,R)\underset{r\to\infty}{\sim}\mathbf{s}(\varepsilon,l,R)+\mathbf{c}(\varepsilon,l,R)\mathbf{Y}(N,E)\ . \tag{42}$$

The diagonal matrices of Coulomb reference wave functions $\underline{s}$ and $\underline{c}$ are constructed to be independent, i.e., $\mathbf{cs}'-\mathbf{c}'\mathbf{s}\equiv1/\pi$, for all R and all channel kinetic energies ε [41]. The analytic properties of these functions has been thoroughly studied by Seaton [42]. Both $\mathbf{s}$ and $\mathbf{c}$ asymptotically approach well-behaved standing waves, and, if all channels are open, the scattering matrix is simply given by

$$\mathbf{S}=(\mathbf{1}+i\mathbf{Y})/(\mathbf{1}-i\mathbf{Y}) . \tag{43}$$

However, at energies below threshold ($\varepsilon=-1/2\nu^2<0$) both functions diverge asymptotically, and we must transform the solutions (42) as follows to obtain (41):

$$\begin{bmatrix}\mathbf{F}_{00}(\mathbf{S})\\ \mathbf{F}_{C0}(\mathbf{S})\end{bmatrix}=\mathbf{F}(\mathbf{Y};N,E,R)\begin{bmatrix}\mathbf{M}_{00}\\ \mathbf{M}_{C0}\end{bmatrix} \tag{44}$$

where

$$\mathbf{M}_{00}=(\mathbf{1}-i\mathbf{R})^{-1} , \tag{45}$$

$$\mathbf{M}_{C0}=-(\tan\boldsymbol{\nu}_C+\mathbf{Y}_{CC})^{-1}\mathbf{Y}_{C0}(\mathbf{1}-i\mathbf{R})^{-1} . \tag{46}$$

$\mathbf{R}$ is the usual $N_0\times N_0$ reactance matrix we would associate with the resonance enhanced scattering matrix $\mathbf{S}=(\mathbf{1}+i\mathbf{R})/(\mathbf{1}-i\mathbf{R})$ which is obtained by eliminating divergent closed-channel components [27] from Eq. (42)

$$\mathbf{R}=\mathbf{Y}_{00}-\mathbf{Y}_{0C}(\tan\boldsymbol{\nu}_C+\mathbf{Y}_{CC})^{-1}\mathbf{Y}_{C0} . \tag{47}$$

Asymptotically the solution vectors in Eq. (44) achieve the following form:

$$\begin{bmatrix}\mathbf{F}_{00}(\mathbf{S})\\ \mathbf{F}_{C0}(\mathbf{S})\end{bmatrix}\sim\begin{bmatrix}(\mathbf{s}_0+\mathbf{c}_0\mathbf{R})\mathbf{M}_{00}\\ (-\mathbf{B}_C\boldsymbol{\beta}_C)\mathbf{M}_{C0}\end{bmatrix} \tag{48}$$

where $\mathbf{B}_C$ is a diagonal matrix of coefficients $B(\nu)=N(\nu)K(\nu)/\cos(\pi\nu)$, with $N(\nu)=(-1)^l(\nu^3/2)^{1/2}$ and $K(\nu)=[\nu^2\Gamma(\nu+l+1)(\Gamma(\nu-l)]^{-1/2}$. The function $\beta_c(R)$ represents that linear combination of s_c and c_c reference Coulomb functions which just cancels their asymptotic diverging components for $\varepsilon<0$ and thus ensures that β_c decays exponentially as $R\to\infty$.

$$\sin(\pi\nu)c(R)-\cos(\pi\nu)s(R)\equiv N(\nu)K(\nu)\beta(R) \sim NK(2R/\nu)^{\nu}\exp(-R/\nu) . \tag{49}$$

We will now introduce (48) into Eq. (22b), and assume that the hydrogen atom is initially prepared in one particular channel state $\theta_c\equiv\theta_{0\gamma}$ within the set of closed channels $\{\theta_c\}$, as in (19b). In this case $\gamma=lm$ simply designates the angular momentum quantum numbers of the bound electron. Further we shall assume that $\mathcal{P}^0_{c,i}$ represents a specific Rydberg level $i=q$ of the unperturbed hydrogen atom, with the *integer* q determined by the condition that $\sin(\pi\nu)=0$, or $\nu=q$ in Eq. (49). (We use q in place of the conventional notation n to avoid confusion with the photon Floquet number n). The larger q, the closer this Rydberg level lies near the ionization limit ($\varepsilon_q=-1/q^2\to0$) and the more reasonable it is to assume that the matrix $\mathbf{Y}(E)$ is essentially constant. The initial normalized radial function takes the following form:

$$\mathcal{P}^0_{c,q}=(-1)^{q+1}N(q)^{-1}s(\varepsilon_q,l,R)\equiv K(q)\beta(q,l,R) . \tag{50}$$

Introducing (48) and (50) into (22b) we obtain

$$C_{o\leftarrow i}=M^*_{c,o}(\nu)O_q(\nu) \tag{51}$$

where

$$O_q(\nu)=[N(\nu)K(\nu)(-1)^q/N(q)\cos(\pi\nu)]\langle\beta(\nu)|s(q)\rangle . \tag{52}$$

The integral between the well-behaved radial function $s(q)$ at energy ε_q and the function $\beta(\nu)$ at energy ε which generally diverges as $R\to0$ can be evaluated using integration by parts:

$$(\varepsilon_q-\varepsilon)\langle\beta|s\rangle\equiv(s\beta'-\beta s')_{R\to0}^{R=\infty}=-(s\beta'-\beta s')_{R\to0}$$

yielding

$$\langle\beta|s\rangle=(s\beta'-\beta s')_{R\to0}/(\varepsilon-\varepsilon_q) . \tag{53}$$

Using the limiting form for $\beta(\nu,R)$ as $R\to0$ and restrict-

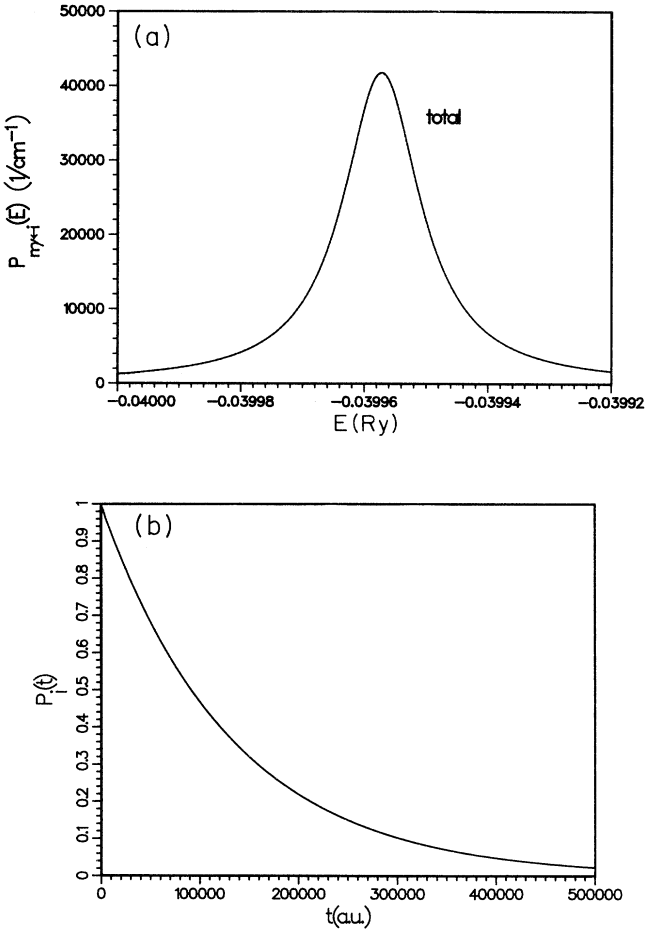

FIG. 4. (a) Probability distribution per unit energy of photoelectrons from H(5s) for $\lambda=364.5$ nm, with circular polarization, and intensity $I=1.7\times10^{11}$ W/cm^2. The kinetic energy ε_n of the electrons produced by the absorption of n photons is $\varepsilon_n=E+n\hbar\omega$. The total probability distribution $\sum_n P_{n\gamma\leftarrow i}(E)$, which is dominated by $n=1$ in this case, is almost perfectly Lorentzian with a total width $\Gamma_i=1.53\times10^{-5}$ Ry, and predicts a pure exponential decay of the initial state, with an ionization rate of 3.15×10^{11} s^{-1}. (b) The probability of the half-collision wave packet remaining in the initial state exhibits a perfect exponential decay with a decay time of 1.31×10^5 a.u. (or 3.17 ps).

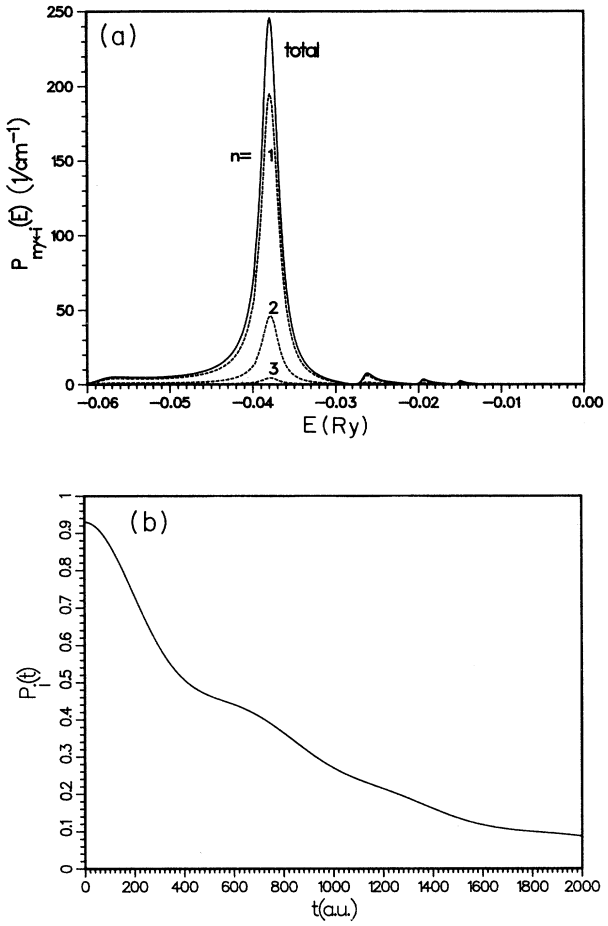

FIG. 5. Same conditions as Fig. 3, but with $I=2.7\times10^{13}$ W/cm^2. (a) The line shape is no longer Lorentzian, and the initial H(5s) Rydberg state produces a wave packet which overlaps and "populates" adjacent Rydberg levels. (b) The resultant decay of the initial-state population is nonexponential. See comments in the caption of Fig. 2 regarding the initial depletion of the population at $t\approx0$.

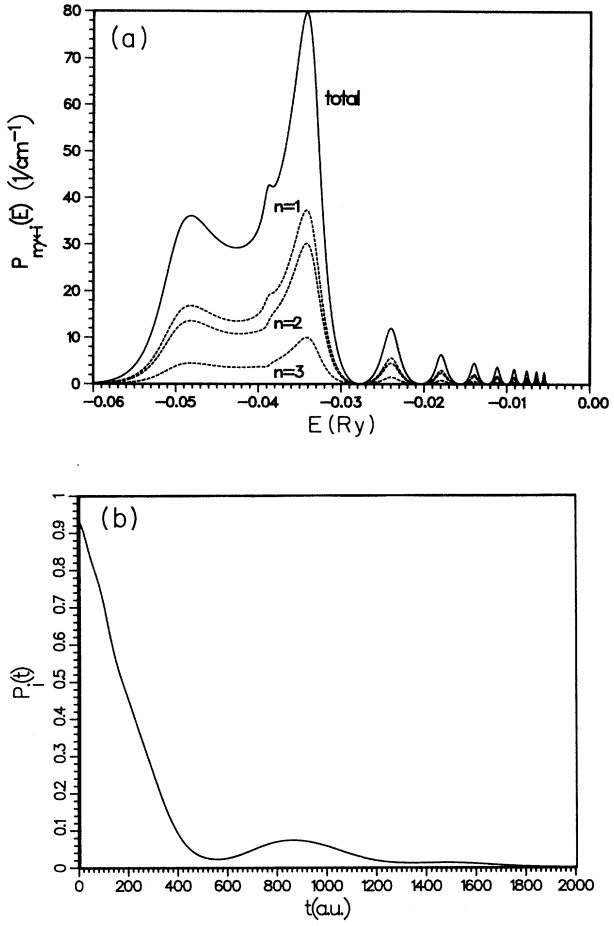

FIG. 6. Same as Fig. 4, but with $I=1.0\times10^{14}$ W/cm^2.

ing ourselves to the special case we will be presenting below, with an $l=0$ initial Rydberg level, Eq. (52) simplifies to the following expression:

$$O_q=\frac{\tan(\pi\nu)}{\pi(\varepsilon-\varepsilon_q)}(-1)^q(q^3/2)^{-1/2}\ . \tag{54}$$

The energy distribution of the photoelectrons originating from the photoionization of H(q,s) into the outgoing γn channel is given by Eq. (24) and simplifies to

$$P_{\gamma n\leftarrow cq}=|\tilde{M}^*_{\gamma n,c}|^2\frac{\tan^2(\pi\nu)}{[\pi(\varepsilon-\varepsilon_q)]^2}(2/q^3) \tag{55}$$

with $M^*_{c,n\gamma}$ a matrix element obtained from the MQDT expression (46). These line shapes are shown in Figs. 4–6 for an initial Rydberg level with $q=5$ in circularly polarized light of wavelength 364.5 nm and different intensities. The numerical values of the Y matrix elements in Eqs. (42) are taken from the close-coupled calculations of Ref. [2]. More recent calculations [43] have demonstrated the possible significance of adding strongly closed channels (corresponding to the ground and first excited Rydberg states of H) to the previous calculations. Nevertheless, Figs. 5 and 6 demonstrate that the MQDT analysis of a half-collision process described by decaying wave packets applies to strongly broadened overlapping resonances and results in a distinctly nonexponential decay. For the lowest intensity, the line shape in Fig. 4(a) is almost perfectly Lorentzian, as for H_2^+ in Fig. 1. The resonance width and shift obtained in this case from Eq. (26) are in excellent agreement with the MQDT expressions derived within the isolated resonance approximation [2].

The expression (55) is a very specialized result, that is only applicable to high-lying Rydberg levels, with $l=0$, and is well designed for the conditions in Ref. [2] which use a MQDT extrapolation across the ionization threshold. In calculation originating for the ground or first excited states, as in Ref. [43], an explicit MQDT analysis can still be used in the perturbative limit, since the initial bound state is still well defined, and approximated by the unperturbed Rydberg states of hydrogen. As the intensity increases, and the overlapping effects that we have demonstrated become significant, especially for lowest

levels, it is probably preferable to forgo the MQDT analysis and use the explicit numerical techniques employed in Sec. V for the photodissociation of H_2^+. One must then evaluate the matrix element in Eq. (22b) at each energy E using explicit numerical integration with the close-coupled solution vectors. However, since in this limit the decay rates may begin to approach the laser frequency, one must be careful not to violate the assumptions involved in averaging over an optical cycle, which is implied, both in our full quantal approach, and in the usual derivation of the Floquet ansatz. If this regime is approached it would be advisable to use explicit solutions to the time-dependent Schrödinger equation [3,8,20,44].

ACKNOWLEDGMENTS

We acknowledge with appreciation many helpful discussions with Rob Heather. Research supported in part by a NATO grant for International Collaboration in Research. One of us (F.H.M.) acknowledges that this work was sponsored in part by the U.S. Air Force Office of Scientific Research.

[1] S.-I. Chu and W. P. Reinhardt, Phys. Lett. **39**, 1195 (1977); S.-I. Chu and J. Cooper, Phys. Rev. A **32**, 2769 (1985).

[2] A. Giusti-Suzor and P. Zoller, Phys. Rev. A **36**, 5178 (1987).

[3] J.N. Bardsley, A. Szöke, and M. J. Comella, J. Phys. B **21**, 3899 (1988); J. N. Bardsley and M. J. Comella, Phys. Rev. A **39**, 2252 (1989).

[4] M. Crance, J. Phys. B **21**, 2697 (1988).

[5] R. Shakeshaft and X. Tang, Phys. Rev. A **36**, 3193 (1987); R. M. Potvliege and R. Shakeshaft, *ibid.* **38**, 4597 (1988); **41**, 1609 (1990).

[6] A. D. Bandrauk and M. L. Sink, J. Chem. Phys. **74**, 1110 (1981).

[7] S.-I. Chu, J. Chem. Phys. **75**, 2215 (1981).

[8] R. Heather and H. Metiu, J. Chem. Phys. **88**, 5495 (1988).

[9] X. He, O. Atabek, and A. Giusti-Suzor, Phys. Rev. A **38**, 5586 (1988).

[10] For pulses times in excess of several hundred femtoseconds we can generally utilize an adiabatic following approximation [3], and treat the amplitude of the electric field $\bar{\mathbf{E}}$ as a constant in time. A subsequent average over the resultant intensity-dependent rate constants can then be performed to conform to the intensity distribution in a given pulse.

[11] S.-I. Chu, Adv. Chem. Phys. **73**, 739 (1989); in *Advances Atomic and Molecular Physics* (edited by D. Bates and B. Bederson (Academics, New York, 1985), Vol. **21**, p. 197.

[12] Quantities such as the wave function $\bar{\Psi}_i$ which are implicit functions of classical electric field strength $\bar{\mathbf{E}}$ will often have an overbar.

[13] L. Dimou and F. H. M. Faisal, Phys. Rev. Lett. **59**, 872 (1987).

[14] When we consider MPD in Eq. (2) the coordinate R represents the internuclear radial coordinate of the separating atomic fragments, while the vector $\mathbf{x}$ in the channel state wave function $\psi_\gamma(\mathbf{x})$ represents all remaining internal degrees of freedom of the molecule, which includes both the fragmentation angular coordinates $\hat{\mathbf{R}}$, and the composite of all electron spatial $\mathbf{r}_e$ and spin $\hat{\mathbf{s}}_e$ coordinates. When we treat MPI in Eq. (1), r is the radial coordinate of the photoelectron, and the channel states $\psi_\gamma(\mathbf{x}) \equiv \sigma_\alpha(\hat{\mathbf{s}}_e) Y_{l,m}(\hat{\mathbf{R}})$ simply designate the spin ($\alpha = \pm\frac{1}{2}$) and radial angular momentum state (l,m) of the ejected electron. As usual in scattering theory we expand in a *complete* set of channel states $\psi_{\gamma'}(\mathbf{x})$ which span the space $\mathbf{x}$.

[15] J. H. Shirley, Phys. Rev. **138**, B979 (1965).

[16] W. H. Louisell, *Quantum Statistical Properties of Radiation* (Wiley, New York, 1973); R. Loudon, *The Quantum Theory of Light* (Clarendon, Oxford, 1973).

[17] H. W. Lee, P. L. DeVries, I. H. Zimmerman, and T. F. George, Mol. Phys. **36**, 1693 (1978).

[18] P. Brumer and M. Shapiro, Chem. Phys. **139**, 221 (1989).

[19] F. H. Mies and M. Krauss, J. Chem. Phys. **45**, 4455 (1966).

[20] R. Heather and F. H. Mies, following paper Phys. Rev. **44**, 7560 (1991).

[21] F. H. Mies, in *Theoretical Chemistry; Advances and Perspectives,* edited by D. Henderson (Academic, New York, 1981), pp. 127–198.

[22] M. H. Mittleman, *Theory of Laser-Atom Interactions* (Plenum, New York, 1982).

[23] We have already tacitly assumed that the center-of-mass motion defined by the momentum wave function $\exp(i\mathbf{k}_{\text{c.m.}} \cdot \mathbf{R}_{\text{c.m.}})/V^{1/2}$ has been factored from Eq. (8) and remains essentially a constant of the motion during the laser-induced process. This is the basis of the dipole approximation, and great care must be taken to choose a gauge which justifies this assumption. In particular, if we truncate the channel state expansion in (8) we must be assured that the remaining basis is sufficient to define all the asymptotic *observable* properties of the scattered fragments.

[24] Scattering channel states must represent asymptotic eigenstates of a *separable* molecule-field Hamiltonian with eigenvalues that are subject to *laboratory observation.* In the dipole approximation the electric field (length) gauge violates this criterion, since, for both processes (1) and (2) the off-diagonal matrix element $\langle \theta_{n\gamma} | V_{\text{rad}} | \theta_{n\pm1,\gamma'} \rangle$ diverges linearly in the coordinate r. Using the Coulomb gauge expression in Eq. (11) ensures that $\langle \theta_{n\gamma} | V_{\text{rad}} | \theta_{n'\gamma'} \rangle$ is asymptotically diagonal and $\theta_{n\gamma}$ represent proper channel states. (Actually, in addition to defining the diagonal ponderomotive potential, $U_P = \langle \theta_{n\gamma} | (e/mc)^2 \mathbf{A}^2/2 | \theta_{n\gamma} \rangle$ the $\mathbf{A}\cdot\mathbf{A}$ operator introduces $|n-n'|=2$ couplings [25] $\langle \theta_{n\gamma} | (e/mc)^2 \mathbf{A}^2/2 | \theta_{n\pm2,\gamma} \rangle/2$ which are generally ignored since they are diagonal with respect to the particle channel states ψ_γ.)

[25] R. E. Moss, *Advanced Molecular Quantum Mechanics* (Chapman and Hall, London, 1973), Chap. 13.

[26] We can envision other experiments wher Θ_v^N is "prepared" by some previous interaction with the laser, such as resonant four-photon ionization [27] of ground state H_2 to form H_2^+ in Eq. (2), and the initial state now initially "dressed" by the laser field which is already active at $t=0$ when the ion is formed by ionization. Such an initial state is not nearly so easily defined.

[27] D. Normand, C. Cornaggia, and J. Morellec, J. Phys. B **19**, 2881 (1986).

[28] S. J. Singer, S. Lee, K. F. Freed, and Y. B. Band, J. Chem. Phys. **87**, 4762 (1987); S. J. Singer, S. Lee, and K. F. Freed, *ibid.* **91**, 240 (1989).

[29] This time-independnet behavior is an artifact of keeping the laser on indefinitely. Once the field is terminated at some distant time $t \gg 0$, the states $\Theta_{n\gamma}(N,E)$ are no longer exact, and these solutions become nonstationary as well. In the limit of infinite depletion of the initial state $\Omega_i(N,t)$ as $t \rightarrow \infty$, and assuming we have chosen a gauge which avoids any radiative interactions in the limit of infinite separation of the fragments, the total probability integrated over all time of observing fragments in channel state γ, with relative kinetic energy $\varepsilon_{n\gamma} = E - E_\gamma - n\hbar\omega$, is given by Eq. (14).

[30] A. Giusti-Suzor, X. He, O. Atabek, and F. H. Mies, Phys. Rev. Lett. **64**, 515 (1990).

[31] W. Heitler, *The Quantum Theory of Radiation,* 3rd ed. (Oxford, London, 1954), pp. 163–174.

[32] D. R. Bates, J. Chem. Phys. **19**, 1122 (1951).

[33] M. K. Chakrabarti, S. S. Bhattacharyya, and S. Saha, J. Phys. B **21**, 3717 (1988).

[34] As shown by L. Pan, L. Armstrong, Jr., and J. H. Eberly, J. Opt. Soc. Am. B **3**, 1319 (1986), the diagonal expectation value of the ponderomotive potential term $\mathbf{A}\cdot\mathbf{A}$ for H(1*S*) exactly cancels the infinite set of second-order terms associated with the $\mathbf{p}\cdot\mathbf{A}$ term. However, in most instances, especially in molecular systems, we include only a limited basis of channel functions $\psi_\gamma(\mathbf{x})$ which may be insufficient to span the coordinate space $\mathbf{x}$. Since we do not include any excited electronic states in our calculations it would be inadvisable to include the $\mathbf{A}\cdot\mathbf{A}$ operator in (11). This points to an important criterion in choosing a gauge to describe a particular problem.

[35] C. Cohen-Tannoudji, J. Dupont-Roc, and G. Grynberg, *Photons and Atoms* (Wiley, New York, 1989).

[36] Harm G. Muller (private communication). Conclusion based on as yet unpublished calculations which show the much more rapid convergence of the adiabatic dressed-state potentials using length rather than velocity couplings to the excited electronic states of H_2^+, at least in the vicinity of $R \approx 2$ a.u.

[37] A. Zavriyev, P. H. Bucksbaum, H. G. Muller, and D. W. Schumacher, Phys. Rev. A **42**, 5500 (1990).

[38] As mentioned in Ref. [30], a linearly polarized laser will result in a preferential dissociation of the fragments along the electric field vector. An explicit analysis of these effects is planned to be presented in a future publication.

[39] The complex energy algorithms are not restricted to just evaluating the total rate, and branching ratios can be extracted. See, for example, Refs. [4] and [5], where such quantiteis are obtained for photoionization of H. However, these procedures are restricted to "interpretating" the imaginary portion of the eigenvalue as a purely exponential decay constant.

[40] G. Alber and P. Zoller, Phys. Rep. **199**, 231 (1991).

[41] For simplicity we set $\hbar^2/m_e \equiv 1$, and replace our previous variables with the usual dimensionless variables of MQDT; $\varepsilon \rightarrow \varepsilon/(e^2/2a_0)$, $R \rightarrow R/a_0$, $k = ka_0$, and $\varepsilon \rightarrow k^2$.

[42] M. J. Seaton, Rep. Prog. Phys. **46**, 167 (1983); J. Dubau and M. J. Seaton, J. Phys. B **17**, 381 (1984).

[43] P. Marte and P. Zoller, Phys. Rev. A **43**, 1512 (1991).

[44] K. C. Kulander, Phys. Rev. A **35**, 445 (1987).